

Dynamic and kinetic aspects of the adsorption of acrylonitrile on Si(001)-2×1

S. Rangan, S. Kubsky, J.-J. Gallet, F. Bournel, K. Le Guen, G. Dufour, and F. Rochet*

Laboratoire de Chimie Physique Matière et Rayonnement, Université Pierre et Marie Curie, 11 rue Pierre et Marie Curie, 75231 Paris Cedex 05, France

R. Funke, M. Knepe, G. Piaszenski, and U. Köhler

Fakultät für Physik und Astronomie, Institut für Experimentalphysik IV/AG Oberflächenphysik, Ruhr-Universität Bochum, NB 4/166, D-44780 Bochum, Germany

F. Sirotti

Laboratoire pour l'Utilisation du Rayonnement Electromagnétique, Centre Universitaire Paris-Sud, Batiment 209D, 91405 Orsay Cedex, France

(Received 19 October 2004; published 21 March 2005)

Using scanning tunnelling microscopy (STM), photoelectron and photoabsorption spectroscopies, we have examined how acrylonitrile ($\text{H}_2\text{C}=\text{CH}-\text{C}\equiv\text{N}$) reacts with the Si(001)-2×1 surface for coverages ranging from $\sim 10^{12}$ molecules/cm² to $\sim 10^{14}$ molecules/cm². At 300 K, in the very low coverage regime (below 10^{13} molecules/cm²), filled- and empty-state STM images show that the molecule bridges, *via* its β carbon and nitrogen ends, two silicon dangling bonds, across the trench separating two dimer rows. A cumulative-double-bond unit ($\text{C}=\text{C}=\text{N}$) is formed. The 300 K STM image results from the dynamic flipping of the molecule between two equivalent equilibrium positions, which can be seen when the molecular motion is slowed down at 80 K. For coverages larger than 10^{13} molecules/cm², for which STM does not show ordered adsorption any more, the adsorption kinetics were observed in real-time using valence band photoemission and resonant Auger yield, associated with N 1s x-ray absorption spectroscopy (NEXAFS). At 300 K, these techniques point to a situation more complex than the one explored by STM at very low coverage. Three species (cyano-bonded, vinyl-bonded, and cumulative-double-bond species) are detected. Their distribution does not vary with increasing coverage. All dimerization-related surface states are quenched at saturation. The uptake rates versus coverage relationship points to the presence of a mobile precursor. Finally, the paper discusses a possible mechanism leading to the formation of cross-trench $\text{C}=\text{C}=\text{N}$ unit at low coverage, and the reasons why the product branching ratio changes with increasing coverage.

DOI: 10.1103/PhysRevB.71.125320

PACS number(s): 68.37.Ef, 68.47.Fg, 68.43.Fg, 61.10.Ht

I. INTRODUCTION

A particularly active field in surface science is the study of the reaction of π -bonded molecules (possessing vinyl, acetylenic or cyano units) with the dimers of the Si(001)-2×1 surface. Understanding the reaction mechanisms paves the way to the controlled growth of organic arrays on Si, with potentially interesting electronic properties.^{1,2} One mechanism leading to molecular adsorption is the opening of a molecular π -bond and the formation of di- σ bonds with a pair a silicon dangling bonds.³ Experimental research efforts were initially aimed at “small” pseudodiatom molecules (acetylene,⁴ ethylene⁵). Attention has now turned towards “larger” *multifunctional* molecules. The objective is to fabricate molecular nanostructures anchored to the silicon substrate by one functional group, leaving the others free to assume a specific role. In that respect, the reactivity of acrylonitrile, which possesses two π units [vinyl and cyano, see Fig. 1(a)] has been examined recently both experimentally^{6–8} theoretically.^{6,9–13} The acrylonitrile/Si(001) system is complex, due to (i) the presence of two different functionalities and the competition between them, (ii) the conjugation of the π units which allows bond shifts within the molecule, and finally (iii) the multiple adsorption sites constituted by a pair of dangling bonds on

the Si(001)-2×1 surface [Fig. 1(b)]. Note that apart from the direct bonding of $\text{C}=\text{C}$ and $\text{C}\equiv\text{N}$ on the surface [possible bonding geometries are given in Figs. 1(c) and 1(d), conjugation allows the formation of a $\text{C}=\text{C}=\text{N}$ cumulative double bond (CDB) unit: Figs. 1(e) and 1(f) show two such configurations, on sites A and D. Naturally CDB bonding on site B and C should also be considered.

N 1s XPS (x-ray photoelectron spectroscopy) spectra and N 1s NEXAFS (near edge x-ray absorption fine structure spectroscopy¹⁴) spectra of a Si(100)-2×1 surface saturated by acrylonitrile at 300 K have been reported by Bournel *et al.*⁷ NEXAFS spectroscopy indicates that three bonding geometries are present on the surface, a minority adspecies bonded *via* the cyano group, forming an Si-N=C-Si unit, and two majority adspecies, a CDB unit having its $\text{C}=\text{C}=\text{N}$ axis nearly parallel to the surface and a pendent $\text{C}\equiv\text{N}$, resulting from a bonding *via* the vinyl group. N 1s NEXAFS spectra are shown and discussed in more detail in Sec. III B 2.

The observation of various adsorption modes at 300 K seems to be in contradiction with an earlier work by Tao and co-workers using HREELS (high resolution electron energy loss spectroscopy) to study acrylonitrile chemisorbed on Si(001)-2×1 at 110 K and subsequently annealed at 300 K.⁶ These authors proposed that acrylonitrile bonds exclusively

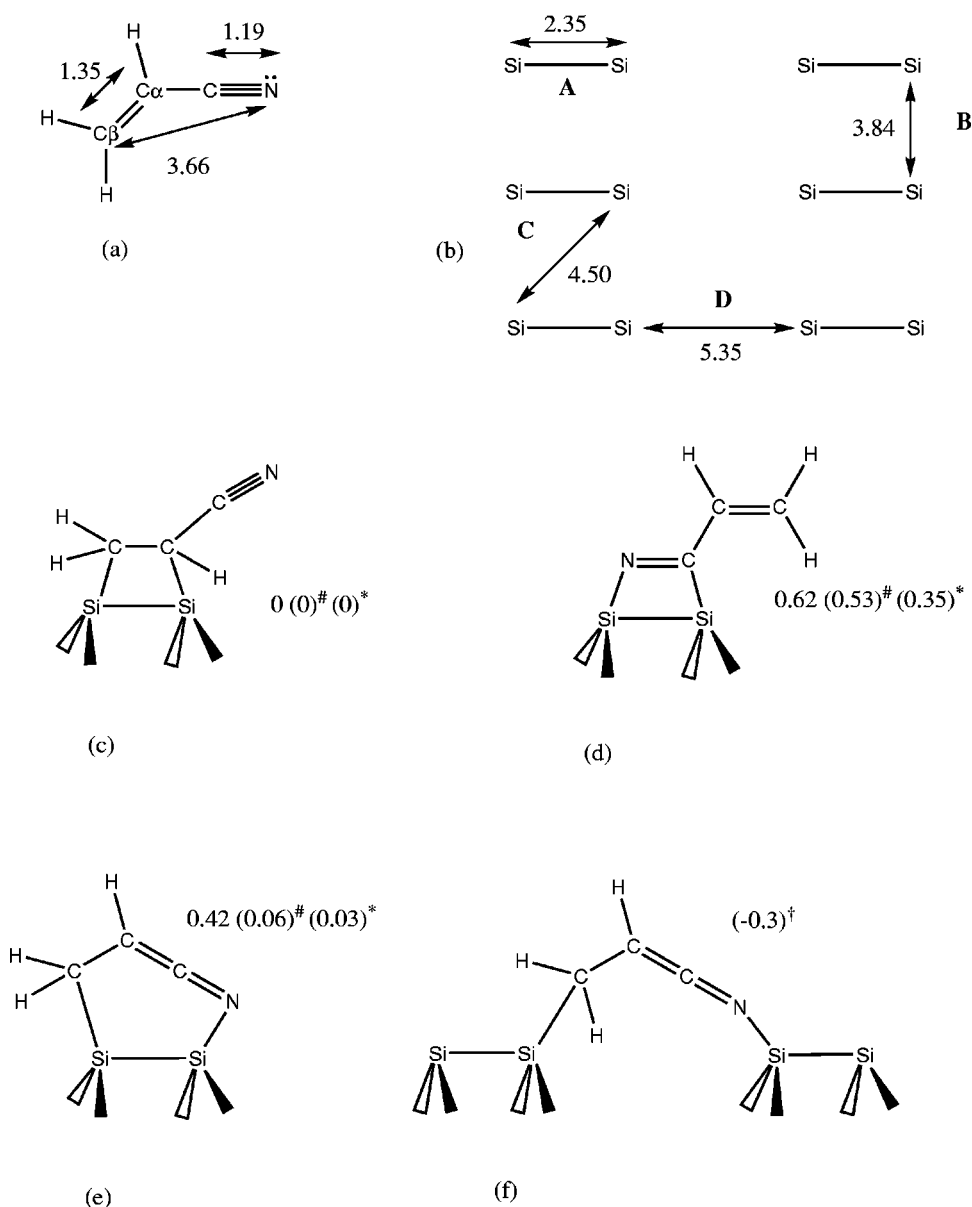


FIG. 1. (a) Acrylonitrile (the bond lengths are given in Å). (b) Possible adsorption sites on Si(001)-2 \times 1, the distances between each pair of dangling bonds are given in Å. (c) Acrylonitrile grafted by the C=C group on site A. (d) Acrylonitrile grafted by the C \equiv N group on site A. (e) CDB geometry on site A. (f) CDB geometry on site D. For geometries (c),(d), and (e) the calculated relative adsorption energies are given in eV [from Choi and Gordon (Ref. 9) [#], from Mui *et al.* (Ref. 10) ^{*}, from Cobian *et al.* (Ref. 11) [†], from Cobian and Boureau (Ref. 12)] with respect to the C=C bound mode on site A (c).

to the silicon dimer via the C \equiv N, as they obtained a C=N stretching mode at 1669 cm⁻¹. However, in the HREELS spectra, there may be also indications of a CDB unit, as a vibrational peak at 2010 cm⁻¹ is seen. Interpreted by Tao and co-workers as a twice CH₂ twist mode,⁶ it is assigned by the same authors to a CDB in the case of acrylonitrile adsorbed on the Si(111)-7 \times 7 surface.¹⁵ Schwartz and Hamers, using MIR (multiple internal reflection)-FTIR (Fourier transform infrared) spectroscopy performed on a surface kept at room temperature, confirm the formation of a CDB with a strong C=C=N absorption peak at 1985 cm⁻¹ and of a pendent C \equiv N (a minority species, a weak mode being found at 2218 cm⁻¹, within the stretching region).⁸

Whereas vibrational and electron spectroscopies all point to the formation of at least three products on the surface (Si-C=N-Si, -C \equiv N, C=C=N), experimental information concerning the adsorption sites [Fig. 1(b)] is lacking. By analogy with ethylene adsorption,¹⁶ C=C bonding with a pair of Si atoms site at A should be preferred to adsorption at

site B. On the other hand, C \equiv N bonding with a Si pair could involve both sites A and B, by analogy with acetonitrile adsorption.¹⁷ As stated before, a CDB unit could appear on sites A, B, C or D.

Various methods are used to perform theoretical calculations of adsorption energies for optimized geometries, "post Hartree-Fock" by Choi and Gordon,⁹ density functional theory (DFT) applied to Si₉H₁₂ clusters by Mui *et al.*,¹⁰ periodical DFT by Cobian *et al.*,¹¹ Cobian and Boureau¹² and Cho and Kleinman.¹³ References 9–11 agree on the hierarchy of adsorption energies on site A, in order of decreasing stability, we found the C=C adsorption mode, the CDB geometry, and the C \equiv N adsorption mode. The calculation reported by Cobian and Boureau¹² shows that the CDB on site D is more stable than the other configurations (-0.3 eV with respect to the C=C grafting mode), in qualitative agreement with the findings of Cho and Kleinman¹³ who find the CDB more stable by -0.16 eV on site D than on site A. The ad-

sorption energies from these references are indicated in Fig. 1 with respect to the C=C bound mode.

Shifting from thermodynamic to kinetic considerations, we note that the results of Choi and Gordon⁹ and Mui *et al.*¹⁰ differ from that of Cobian *et al.*¹¹ as concerns the reaction path found for C=C anchoring. A large barrier of 0.72 eV (0.44 eV) is calculated by Choi and Gordon⁹ (by Mui *et al.*¹⁰), while no barrier at all is found by Cobian *et al.*¹¹ Experimental work at 300 K shows indeed that C=C anchoring is facile.⁷

Our previous NEXAFS study was indicative of various adsorption configurations on the surface *at saturation coverage*.⁷ The aim of the present work is to combine a local probe, scanning tunnelling microscopy (STM) to the global, but chemically sensitive, XPS and NEXAFS probes, this to examine the adsorption sites, the chemical bonding and the possible variation in the product branching ratios as a function of coverage, in the $\sim 10^{12}$ molecules/cm² to $\sim 10^{14}$ molecules/cm² range. Special attention has been paid to the dynamics of the individual admolecule (by comparing room temperature with low temperature STM results) and to the kinetic aspects (in particular by carrying out *real-time* electron spectroscopy measurements).

II. EXPERIMENTAL DETAILS

A. Scanning tunnelling microscopy

The STM images were obtained under ultrahigh vacuum, operating in a base pressure regime of 10^{-11} mbar. The acrylonitrile was introduced into the STM chamber via a leak-valve after cleaning with several freeze-pump-thaw cycles. Exposures were made at room temperature on freshly cleaned Si(001)- 2×1 samples (see below).

Image sequences showing the dynamic behavior of the adsorption processes were made at room temperature by taking one image per 4 seconds while dosing the surface. Such motion pictures were also obtained at 80 K using a variable temperature STM. For these measurements the surface was cooled down to 80 K after dosing at room temperature.

All STM images presented in this paper were taken in the constant current mode using a tunnel current in the 0.5 nA to 1.5 nA range. Filled and empty states images of the sample were obtained by setting the sample bias voltage negative or positive, respectively. The Si(001) substrates (Sb doped, 0.014 Ω cm resistivity) were prepared under UHV conditions by outgassing at 600 °C for 12 hours and flashing off the surface oxide at 1250 °C, followed by 5–10 additional flashes to 1250 °C. After the final flash the sample was slowly cooled down to room temperature. This procedure results in a clean Si(001)- 2×1 surface with a low density of missing dimer defects.

B. Electron spectroscopies

Electron spectroscopy measurements were performed at the SB7 beamline of SuperACO storage ring (LURE Synchrotron Facility, Orsay, France), using a Dragon type monochromator at a bending magnet.¹⁸ The source was linearly polarized (95%). The main component of the electric field,

contained in the horizontal plane, always laid in a silicon (110) plane. The sample could rotate around a vertical axis, so that the beam incidence angle θ (measured with respect to the sample surface plane) could be changed. θ is also equal to the angle between the main electric field component (**E**) and the normal to the surface. The ABS6/C-Seal end-station used was equipped with a Scienta 200 electron analyzer for XPS and NEXAFS measurements.

The NEXAFS N 1s spectra were taken in the Auger yield mode (KVV transitions) to achieve a good adsorbate sensitivity. Two 18 eV wide kinetic energy windows, centered at 363 and 373 eV, were chosen using the Scienta analyzer in the “fixed” mode. The spectra were normalized with respect to the secondary electron photoemission peak dominated by contributions from bulk Si. The photon bandwidth was 180 meV. Angle dependent measurements were performed by varying θ , between 90° (normal incidence) and 16° (grazing incidence). The photon energy was calibrated using the first and second order light from the monochromator.

NEXAFS intensities were measured during dosing in real-time. We refer to this as real-time “resonant Auger yield” (the Auger kinetic energy window was placed at 363 eV). The gas was introduced at constant pressure directly in the analyzer chamber *via* a leak-valve. The normalization of these data was made by dividing by the NEXAFS intensity below the N 1s edge (395 eV). These measurements were made at $\theta=54.7^\circ$ (the so-called magic angle), in order to suppress any effect due to a possible reorientation with time of the various species.¹⁹

Valence band photoemission spectra were also recorded in real-time with a He I source ($h\nu=21.2$ eV). Photoelectrons were measured in normal emergence, with a 10 eV wide kinetic energy window, in order to follow simultaneously the time evolution of the silicon surface states and of the acrylonitrile molecular states.

Phosphorus doped (0.003 Ω cm resistivity) wafers were used. Their nominal orientation was (001). The surface was cleaned from the native oxide by flashing at 1250 °C, after degassing for 24 hours at 600 °C. The appearance of a two-domain Si(001)- 2×1 reconstruction was checked by low energy electron diffraction.

III. RESULTS AND DISCUSSION

A. Low coverages studied by STM

The images for the filled states measured at 300 K shows that the clean surface dimers have the symmetric shape characteristic of dynamical flipping. While dosing the surface with acrylonitrile, a characteristic signature of the molecule appears on the surface. Figure 2(a) shows a sequence of STM-images during acrylonitrile dosing where the successive adsorption of individual molecules can be seen. The arrows indicate newly adsorbed molecules. In most cases a specific molecular imprint is seen in this initial stage of adsorption. In less than 5% of the adsorption events, the appearance of the imprint differs [like the one marked by the lowest arrow in the lower right-hand frame of Fig. 2(a)]. This is probably caused by cracked molecules. The dominant mo-

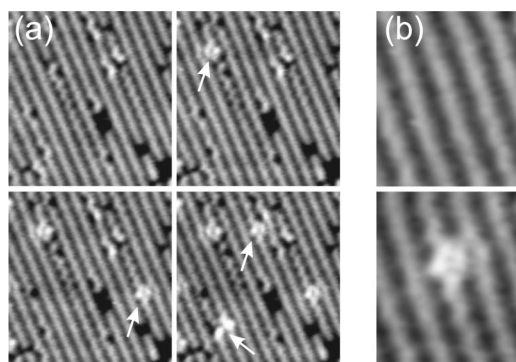


FIG. 2. (a) In-situ STM adsorption sequence (acrylonitrile pressure = 10^{-9} mbar): the time line runs (not linearly) from the upper left to the lower right image. The white arrows indicate newly adsorbed molecules (image size $95 \text{ \AA} \times 110 \text{ \AA}$). (b) Magnified view of an adsorption event, the upper image shows the clean surface before adsorption. The lower image shows the same surface area after an adsorption event which induces a static buckling of one dimer row (image size $35 \text{ \AA} \times 40 \text{ \AA}$). Images in (a) and (b) have been measured at 300 K, with $V_b = -1.7 \text{ V}$ and $I = 0.5 \text{ nA}$.

lecular imprint displays an elongated feature, or barlike feature, between two Si-dimer rows together with a modification in both dimer rows bordering the elongated feature. A strong static buckling is induced in one of the dimer rows which is attenuated over a range of 5–7 dimers [Fig. 2(b)]. Intuitively one can consider that the influence of the adsorbed molecule on dimers pertaining to two adjacent rows provides a strong indication for a cross-trench adsorption mode. At this stage there is no indication of adsorption on a single dimer [site A in Fig. 1(b)].

The minimum distance between two dangling bonds of two adjacent dimer rows is 5.35 \AA [site D, Fig. 1(b)], a distance which would allow the acrylonitrile molecule to bond by its β -carbon and nitrogen atoms with the formation of a CDB, as shown in Fig. 1(f). Atomically resolved images give further insight into the local bonding geometry. An occupied states image of an adsorbed acrylonitrile molecule is shown in Figs. 3(a) and 3(b) ($V_b = -1.7 \text{ V}$ and $I = 1.5 \text{ nA}$). The image shows (i) a barlike feature in the middle of two dimer rows between the silicon atoms #2 and #3, (ii) a depression on silicon #2 and #3, and finally (iii) a protrusion (ball-like structure) above silicon #4. This could be an indication of strong charge transfers between the molecule and the substrate, and/or of variations in the silicon atom heights. In Figs. 3(c) and 3(d), we compare filled-state images (-1.9 V) and empty-state images ($+1.8 \text{ V}$) of one adsorbed molecule. The “protrusion” on Si #4 in the occupied-state image shifts to Si #1 in the empty-state image. This strongly suggests that Si #1 (Si #4) bears an empty (filled) dangling bond.

At a mechanistic level, the room temperature adsorption of acrylonitrile may be described in the following way (Fig. 4). Conjugation allows a mesomeric form depicted in Fig. 4(b) with positive (negative) charge on the β -carbon (nitrogen) atom. The positively charged β -carbon binds to an electron-rich Si atom (an up silicon dimer atom) while the negatively charged nitrogen is attached to an electron-poor Si

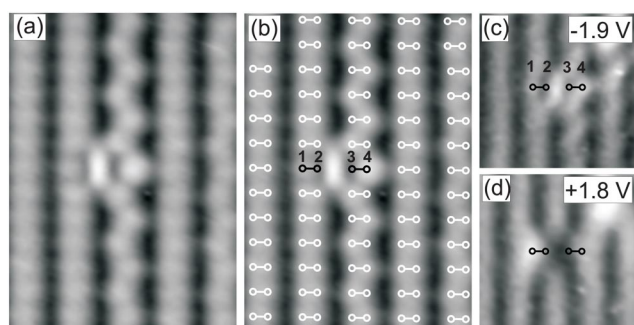


FIG. 3. (a) Atomically resolved occupied-state image (adsorption and measurement at 300 K, $V_b = -1.7 \text{ V}$, $I = 1.5 \text{ nA}$) of an adsorption site. (b) The same image as in (a) with dumb-bells symbolizing the silicon dimers. The molecular imprint shows a barlike feature, placed in the trench separating two dimer rows, and a ball-like feature (on Si-atom #4) together with a static buckling of the dimer row right to the bar-like feature (image size $35 \text{ \AA} \times 50 \text{ \AA}$). (c) Occupied-state ($V_b = -1.9 \text{ V}$, $I = 0.5 \text{ nA}$) and (d) empty-state ($V_b = +1.8 \text{ V}$, $I = 0.5 \text{ nA}$, image size $30 \text{ \AA} \times 30 \text{ \AA}$) images of the same adsorption site. The images suggest that the dangling bond on Si #4 (respectively, on Si #1) possesses a large charge density below the Fermi level (respectively, above the Fermi level).

atom (a down silicon dimer atom) of the adjacent row. The adsorption site must be formed of two adjacent dimer tilted “inphase.” Indeed DFT calculations show that the 2×2 and $c\text{-}4 \times 2$ reconstructions are nearly degenerate in energy.²⁰ The resulting product corresponding to a CDB species is depicted in Fig. 4(c). Within such a Lewis acid-base reaction scheme, the remaining dangling bond on the Si-dimer attached to the nitrogen atom is filled, the one on the dimer attached to the carbon atom is empty.

The barlike feature seen in the occupied states images in between the dimer rows is 9 \AA long, largely exceeding the dimensions of the molecule (3.7 \AA is the distance between the β -carbon and nitrogen atoms in acrylonitrile). Low temperature STM experiments were performed to check if the large size of the molecular imprint at 300 K could be explained by a thermally activated motion of the adsorbate between different configurations. A surface dosed at 300 K (30 s under a pressure of 10^{-9} mbar) was cooled to 80 K, in an attempt to freeze the molecular displacements. Successive STM scans (4 s between two images, $V_b = -3 \text{ V}$, $I = 1 \text{ nA}$) were made imaging one molecule [Fig. 5(a)]. Instead of the large barlike feature in between the dimer rows, a single “protrusion” is now seen flipping between two positions (white arrows) mirrored by a (110) plane containing the Si-Si axes of the dimer pairs involved in the CDB bonding. In Fig. 5(b) we report a Hartree-Fock geometry optimization (STO-3G, Gamess)²¹ of the CDB geometry, showing that the α -hydrogen is separated by about 2 \AA from the mirror plane. If one assumes that the flipping between the two equivalent positions seen at 80 K is thermally activated one can deduce an activation energy barrier of 200 meV from the oscillation frequency in the range of 1 Hz (assuming a prefactor of 10^{13} Hz).

Therefore, the barlike feature in between the Si-dimer rows seen at room temperature is actually an averaged image of the two equilibrium positions of the molecule with respect

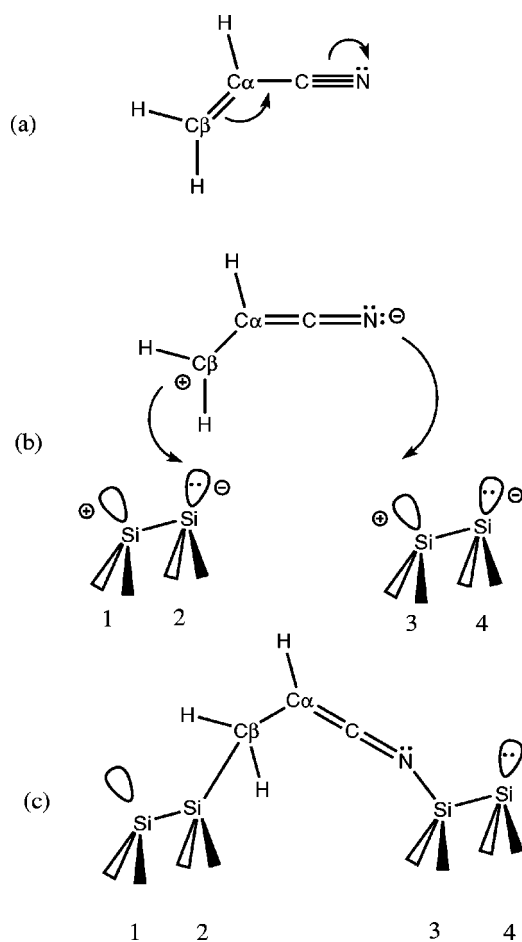


FIG. 4. (a) The mesomeric form of acrylonitrile with opposites charges on its β -C (positively charged) and N (negatively charged) atoms. (b) On the clean surface, the silicon dimers are buckled, electron charge is transferred from the down atom (positively charged) to the up atom (negatively charged). Bonding occurs *via* Lewis acid-base reactions, the basic nitrogen donates electronic charge to the acidic Si #3, while the acidic β -carbon attaches to the basic Si #2. (c) A CDB geometry results, with a filled dangling bond on Si #4 (close to the N-end) and an empty dangling bond on Si #1 (close to the C-end).

to the mirror plane. The above estimated activation energy for a flip between the configurations result in a flipping rate of 3×10^9 Hz at 300 K. To simulate the appearance of the adsorbate in the STM-images taken at 300 K the images of the temporal sequence taken at 80 K were averaged [see Fig. 5(c)]. A barlike feature in between the dimer rows becomes visible, which is in good agreement with the room temperature image of Fig. 3(a). Note however, that at 80 K buckling is seen on both sides of the molecular imprint, likely because the surface temperature is below that of the dynamic-to-static buckling transition (120 K).²²

The STM images of Figs. 2, 3, and 5 correspond to very low coverages (in the 10^{12} molecules/cm² range).²³ In order to examine higher coverages up to surface saturation, in-situ STM experiments of the adsorption were made using the following procedure: (i) the surface was dosed for 4 min under 10^{-9} mbar of acrylonitrile, while the tip was retracted (to avoid screening the surface). Additionally, V_b was set to

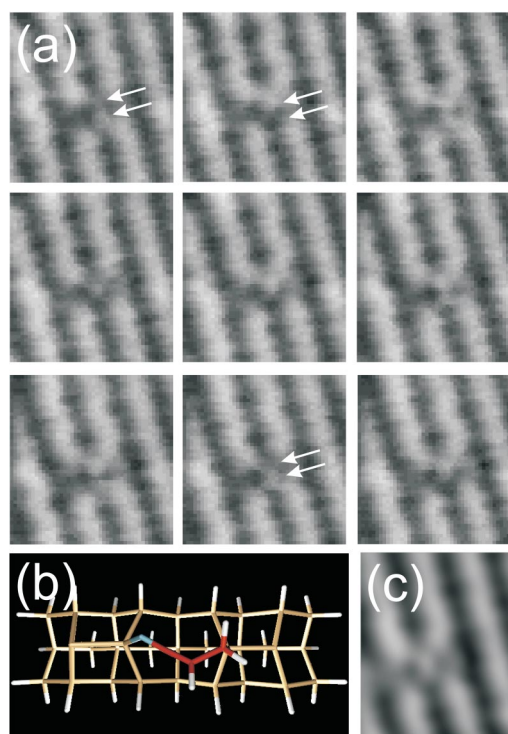


FIG. 5. Occupied-state images ($V_b = -3$ V, $I = 1$ nA, image size $30 \text{ \AA} \times 30 \text{ \AA}$) measured at 80 K after dosing the surface for 30 s under a pressure of 10^{-9} mbar at 300 K. (a) Chronological sequence (4 s/image) showing a single protrusion as the molecular imprint appearing at the positions indicated by the upper (respectively, the lower) white arrow. The time line runs from the upper left to the lower right image. (b) Geometrical optimization of the CDB on a Si₂₂H₁₄ cluster (Gamess, Hartree-Fock, STO3G), the α -H is distant by about 2 \AA from the (110) mirror plane containing the dimer pairs. (c) Average of the temporal sequence of (a).

zero to prevent a deflection of the path of the arriving molecules by the inhomogeneous electrical field between tip and sample. (ii) The leak-valve was closed and an STM image was recorded. This procedure was iterated a number of times. Figure 6 shows a series of images up to a total exposure time of 12 min. After a 4 min exposure, the characteristic image of the CDB adsorption geometry is seen. After an 8 min exposure, the surface looks more disordered. There is no long range order in the adsorbed layer and there is more than one adsorption site involved. Indeed protrusions appear, centered on one dimer row. After a 12 min exposure, it is difficult to identify individual molecules. Multiple adsorption modes in a “disordered way” complicate a detailed analysis of the adsorption configuration by STM.

Therefore, for this system, STM was not used to gain information on the local adsorption modes for molecular coverages above $\sim 10^{13}$ molecules/cm². Instead, we have used real-time resonant Auger yield and real-time UV valence band photoemission (UPS) to examine the distribution of the various adspecies as a function of exposure time (coverage). Information is provided by this method for typical coverages in the 10^{13} to 10^{14} molecules/cm² range.

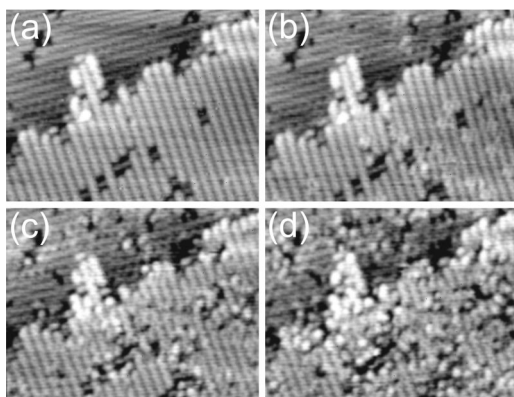


FIG. 6. Occupied-state images sequence (adsorption and measurement at 300 K, $V_b = -1.7$ V, $I = 1.5$ nA (image size $145 \text{ \AA} \times 190 \text{ \AA}$, acrylonitrile pressure 10^{-9} mbar). (a) The clean silicon surface. (b) After 4 min, acrylonitrile adsorbs in a single adsorption mode, a cross-trench CDB. (c) After 8 min, the surface starts to look disordered and the single adsorption mode of image (b) is hardly visible anymore (the coverage is now in the 10^{13} molecules/cm² range). In a few locations an adsorption mode becomes visible where a single protrusion is located on a dimer row. (d) After 12 min, the identification of individual molecules is difficult.

B. The high coverage regime studied by photoemission and x-ray absorption spectroscopies

1. Real-time UPS at 300 K

In order to monitor changes of the valence band upon adsorption, real-time UPS was carried out while dosing acrylonitrile (Fig. 7) at 300 K under a pressure of 2×10^{-9} mbar. We observed a gradual quenching of the surface states situated at a binding energy of 0.85 eV and the growth of a molecular state at 2.2 eV. At saturation (when the molecular states intensity remains constant), the disappearance of all surface states indicates that all silicon dangling bonds are affected by the reaction of acrylonitrile with the surface. The photoemission intensity is integrated over two binding energy windows (0.7 eV wide) centered on the surface states and on the molecular state. The intensities of the two states are plotted in Fig. 8 as a function of time. The quenching rate of the surface states, as well as the growth rate of the molecular state, remain constant up to saturation, indicating a non-Langmuirian process where a mobile molecular precursor intervenes.²⁴ Other measurements were made at different pressures up to 5×10^{-8} mbar, the maximum pressure reachable due to vacuum and spectra-acquisition considerations. The surface state quenching rate r_Q is defined as the ratio $1/\tau_Q$, where $t=0$ is the time at which the gas was introduced, and τ_Q the time at which saturation occurs. The absolute value of r_Q is plotted in Fig. 9 as a function of pressure. Given the error bars, r_Q increases linearly with pressure in accord with the mobile precursor model.²⁴

2. NEXAFS and real-time resonant Auger yield at 300 K

The Auger yield NEXAFS spectra of a Si(001)- 2×1 surface, saturated with acrylonitrile (4650 s under 10^{-8} mbar) at

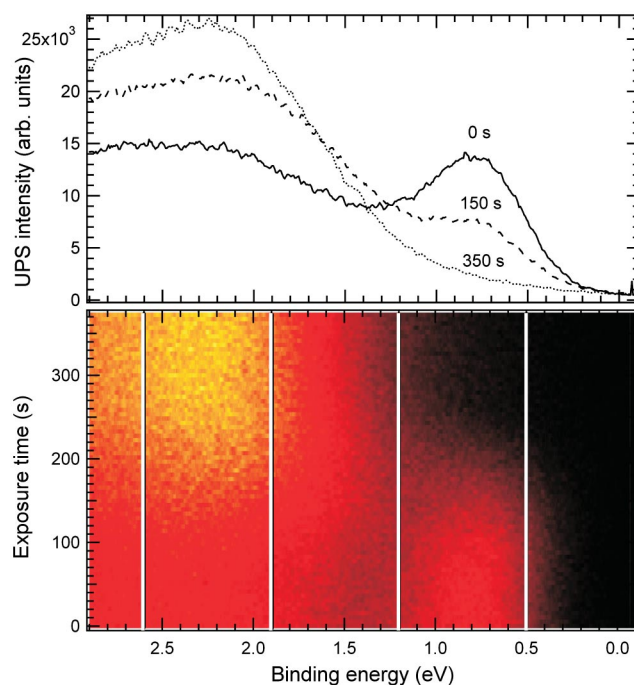


FIG. 7. Real-time UPS (He I) of the Si(001)- 2×1 surface exposed to acrylonitrile at 300 K under a pressure of $2 \cdot 10^{-9}$ mbar. Lower panel, photoemission intensity (reflected in color scale from black (zero) to yellow (10^4 counts)) as a function of binding energy (x -axis) and exposure time (y -axis). Spectra are taken each 7 s. Acrylonitrile is introduced at time zero. The white vertical lines delimit the integration windows of the surface states (centered at a binding energy of 0.85 eV) and of the molecular states (centered at a binding energy of 2.25 eV). The corresponding kinetics are reported in Fig. 8. Higher panel, photoemission intensity versus binding energy at times 0 (pristine surface), 150, and 350 s (saturated surface). The Fermi level is at 0 eV.

300 K are given in Fig. 10 for three values of θ : 90° (normal incidence), 54.7° (magic incidence), and 16° (grazing incidence). The NEXAFS spectra show a first weak $\pi^*(1)$ transition at 397.3 eV, maximum at $\theta=90^\circ$ (plane polarized). This bonding is a minority species, attributed to an anchoring by the $C \equiv N$ group (Fig. 11). Two majority species are de-

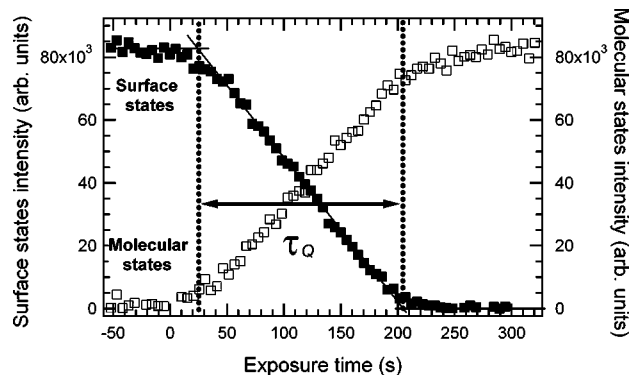


FIG. 8. Integrated photoemission intensities of the surface states (filled squares) and molecular states (empty squares) shown in Fig. 7, plotted as a function of exposure time. All surface states are quenched over a characteristic time τ_Q .

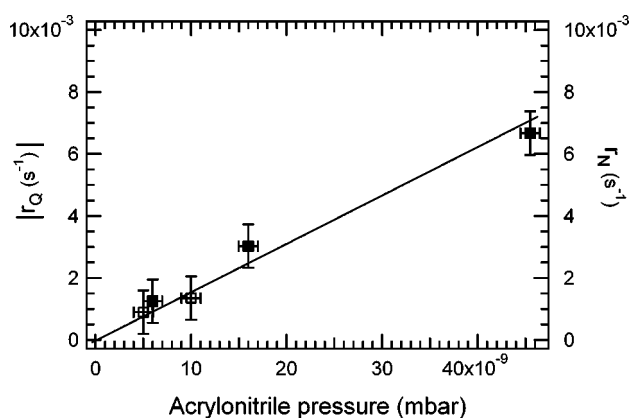


FIG. 9. Surface states quenching rate ($|r_Q|$, filled squares) and nitrogen uptake rate (r_N , empty squares) at 300 K plotted as a function of acrylonitrile pressure.

ected. The first gives rise to two mutually orthogonal transitions, $\pi^*(2)$ peaking at $\theta=90^\circ$ and $\pi^*(4)$ peaking at $\theta=16^\circ$, found at 398.8 and 401.5 eV, respectively. We attribute them to the formation of a CDB (see two lower configurations in Fig. 11). The second is characterized by a weakly dichroic transition $\pi^*(3)$ at 399.4 eV, attributed to an anchoring by the C=C, leaving a pendent C \equiv N (Fig. 11). A recent periodical DFT geometrical optimization of these structures by Cobian *et al.* shows that the C \equiv N axis of the pendent cyano group makes an angle γ of 50° with respect to the normal to the surface.¹¹ This angle is indeed close to 54.7° , an angle for which the NEXAFS angular dependence becomes indistinguishable from that of a randomly oriented molecule, in the case of surfaces of symmetry higher than 3 (the symmetry of the present two-domain surface was fourfold).²⁵

While the N 1s photoelectron spectra do not enable us to separate easily the different contributions of each species, an indication of their relative distribution can be obtained from a fitting of the NEXAFS line intensities measured at magic angle incidence. We find that the intensity ratio $\pi^*(1):(\pi^*(2)+\pi^*(4)):\pi^*(3)$ is 5%:60%:35%. Neglecting cross section variation effects, this ratio would correspond to the distribution of cyano-bonded species, CDB, and vinyl-bonded species, respectively.

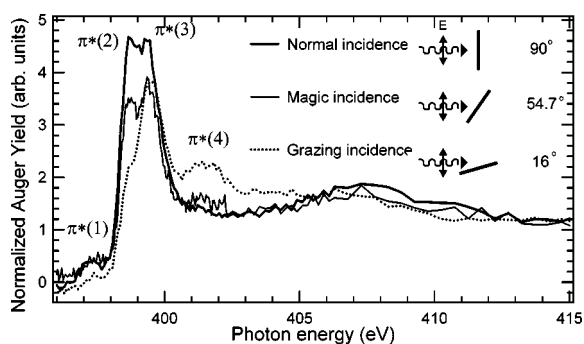


FIG. 10. Angular dependent N 1s NEXAFS spectra of a Si(001)- 2×1 surface saturated with acrylonitrile (at 300 K for 4650 s under 10^{-8} mbar) for three photon beam incidence angles θ [normal (90°), magic (54.7°), and grazing (16°)].

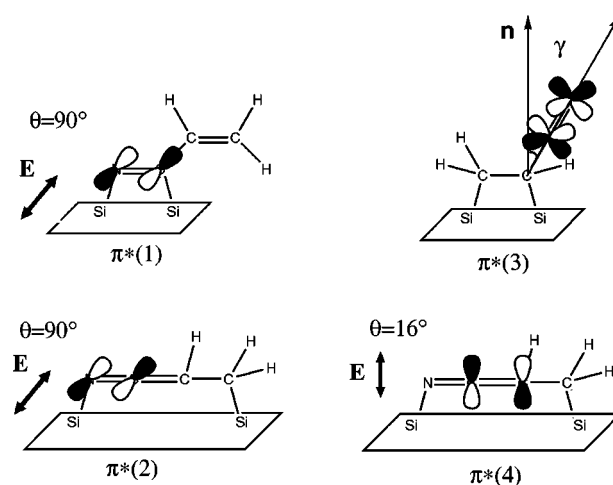


FIG. 11. Schematics of the three adsorption modes of acrylonitrile at 300 K, and of the orientation of their π^* antibonding orbitals. For the vinyl-bonded species, γ is the angle between the normal to the surface (\mathbf{n}) and the C \equiv N axis. \mathbf{E} is the main component of the synchrotron radiation electric field. θ measures the angle between \mathbf{n} and \mathbf{E} . $\pi^*(1)$ and $\pi^*(2)$ transitions will be maximum when $\theta=90^\circ$ (normal incidence), while $\pi^*(4)$ will be maximum when θ is close to 0° (grazing incidence). $\pi^*(3)$ is weakly dichroic, pointing to an angle γ close to 54.7° .

In order to follow the growth of the different adsorption modes, real-time resonant Auger yield measurements (Fig. 12) were performed by monitoring the Auger yield for the three energies corresponding to the three grafting modes of the acrylonitrile, 397.3 eV for the attachment via the cyano

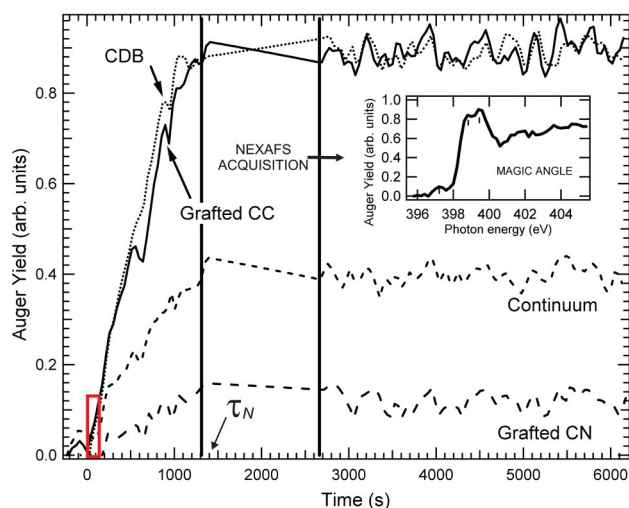


FIG. 12. Real-time resonant Auger yield measurement during gas exposure at 300 K under 5×10^{-9} mbar. The three NEXAFS structures (at 397.3, 398.8, and 399.4 eV), correspond to the three detected adsorption modes (grafted by C \equiv N, CDB, and grafted by C=C, respectively). The Auger yield intensity measured at 415 eV (continuum) is proportional to the amount of nitrogen on the surface. The measurements were made at $\theta=54.7^\circ$ (magic angle). In the inset we show the NEXAFS spectrum taken at saturation. The rectangular box represents a dose (pressure \times time) equivalent to that of the STM image in Fig. 6(d).

group, 398.8 eV for the CDB structure, and 399.4 eV for the attachment by the C=C leaving a pendent C≡N. The Auger yield was also measured far from bound π^* resonances, in the continuum at $h\nu=415$ eV, its intensity is directly proportional to the amount of nitrogen atoms deposited on the surface. The dosage, under a pressure of 5×10^{-9} mbar, has been stopped at saturation (after ~ 1300 s). A NEXAFS spectrum taken just after dosing is also reported in the inset of Fig. 12, a comparison made with Fig. 10 points to a fair experimental reproducibility.

At high coverage NEXAFS detects three different species, while at very low coverage (below 10^{13} molecules/cm²) the CDB geometry is the only adsorption mode that can be detected by STM. The main contribution of resonant Auger yield (Fig. 12) is the observation that *the adspecies distribution does not vary as exposure proceeds*. In order to examine the consistency between data provided by STM and real-time resonant Auger yield, we have drawn in Fig. 12 a “box” representing a dose (exposure time \times pressure) equivalent to that of the STM image in Fig. 6(d), for which STM does not show ordered adsorption any more (this procedure is valid only when the uptake rates are proportional to pressure). Given that the Auger yield intensities of the various adspecies are, within the box, comparable to the experimental noise, it appears that the applicability domains of STM and synchrotron radiation spectroscopies do not overlap, essentially because of the too low photon flux in the latter case. The second information contained in Fig. 12 concerns the growth rates of the three species, and consequently the overall rate of deposited nitrogen. They are found to be constant until saturation is reached (at time τ_N). This again (See sec. III B 1) points to a mobile precursor. A characteristic nitrogen uptake rate r_N (where $r_N=1/\tau_N$) is obtained as a function of pressure, and is displayed additionally in Fig. 9 (see empty squares), together with the absolute value of the surface state quenching rate ($|r_Q|$) measured by real-time valence band photoemission. r_N and $|r_Q|$ lie on the same straight line plotted as a function of pressure.

From valence band photoemission we know that all surface states are quenched at saturation coverage. Therefore, the adsorption models must be compatible with this observation, both in terms of chemical bonding and of surface site filling. Bonding on a single dimer [see site A in Fig. 1(b)] via C=C and C≡N is quite effective as it leads to the elimination of the Si-Si π state from the surface gap. If the CDB bonding on site D leads to an empty dangling bond on silicon #1 and to a filled dangling bond on silicon #4 [as depicted in Fig. 4(c)], then the filled dangling bond state must be degenerate in energy with bulk silicon levels. Moreover there is no self-avoidance between adspecies, due to, e.g., electronic repulsion, so that silicon dimers remain nonreacted.

The distribution of the different species was also followed for hours after surface saturation is reached (i.e., when a constant amount of nitrogen on the surface is reached). This was to detect possible geometry rearrangements after adsorption. Indeed, desorption or “bond-cracking” events have been occasionally observed under the tip during STM scannings. Isomerization paths between a vinyl-bonded species and a cyano-bonded one, going through a CDB product on an A site, are unlikely, due to the very large activation barriers

(~ 1.7 eV).⁹ On the other hand, other transformations, involving more than one dimer site, can be envisaged. For instance, the “cross-trench” CDB could become detached at the N end to evolve towards a bonding *via* the C=C moiety, or to the formation of a CDB on site B (the Si- β C bond would remain unchanged). Analogously to the benzene case,²⁶ the nitrogen end of a pendent C≡N could react with a close neighbor silicon dangling bond, pertaining to a non-reacted adjacent dimer in the same row.²⁷ Examination of Fig. 12 clearly shows that the distribution of the various adspecies, after surface saturation, does not change with time, because of kinetic considerations (barrier heights) and/or of site occupation on the surface, i.e., no sites being available for a transformation.

IV. CONCLUSION

The combined use of STM and (real-time) electron spectroscopies have enabled us to determine the adsorption sites and the chemical bonding of products resulting from the reaction of acrylonitrile, a conjugated π molecule, with the Si(001)- 2×1 surface.

When the molecule is deposited at 300 K, only one adsorption geometry is observed by STM in the very low coverage regime (coverage less than 10^{13} molecules/cm²). To account for the filled- and empty-state images, we propose that a cumulative double bond (CDB) unit bridges two silicon dangling bonds over the trench separating two dimer rows (*via* its nitrogen and β carbon). By construction, the cross-trench CDB (CDB on site D) has two symmetry equivalent equilibrium positions, that we have been able to image by slowing down the molecule back-and-forth motion at 80 K. Adsorption at 300 K induces also a strong static buckling in only one of the two bridged dimer rows, pointing to an asymmetry in the charge transfer resulting either from Si-N or Si- β C bond making. The simple picture we give of the reaction path, leading the formation of a CDB, is based on a Lewis acid-base reaction scheme. It emphasizes both the role of dynamic dimer buckling at 300 K and the polarity of the molecule, allowed by conjugation.

For coverages larger than 10^{13} molecules/cm², STM performed at 300 K pointed out multiple adsorption modes, but could not provide precise information on local bonding geometries. Therefore, we lack indications about the perturbation of the surface electronic structure around a CDB site and its influence on reactivity. For instance, what is the reactivity of empty and filled silicon dangling bonds (atoms #1 and #4 in Fig. 3) with another molecule? Other problems related to dimer buckling may arise. As depicted in Fig. 4 the insertion of a cross-trench CDB in a D site needs a pair of silicon dimers which are buckled “inphase.” Dynamic buckling allows such an occurrence, as long as adspecies are sufficiently apart. As the surface is more and more crowded, the consequence of static buckling (which extends over ~ 20 Å along a dimer row) could be that more and more D sites have dimer pairs statically buckled out of phase. This frustration may alter (i.e., increase) the energy barrier leading to the formation of a cross-trench CDB. Therefore geometries other than the cross-trench CDB may be kinetically favored,²⁸ not to

mention cases in which one dimer remains isolated, on which only bonding *via* C=C or C≡N is possible.

The fact that the situation may gain in complexity with increasing coverage is indeed confirmed by NEXAFS and real-time resonant Auger spectroscopies. Due to a limitation of the photon flux, the spectroscopic methods can only provide an insight into adsorbate bonding from a coverage of $\sim 10^{13}$ molecules/cm². Unfortunately there is no overlap yet with the coverage range studied by atomically resolved STM. Kinetic studies performed at 300 K show that the relative distribution of the three observed species, the minority cyano-bonded adspecies, and the two majority species, the vinyl-bonded and the CDB adspecies, does not vary during the adsorption process. In contrast to a previous vibrational study,⁸ CDB and vinyl-bonded species are found by N 1s NEXAFS in comparable amounts. Real-time valence band spectroscopy shows also that surface saturation coincides with the consumption of all Si dimer π states. This information is crucial for the modelling of acrylonitrile adsorption at room temperature.

We expect this work will lead to further experimental and theoretical work being done. On the experimental side, high resolution STM imaging conditions remain to be found at high coverage, for which multiple adsorption geometries are detected by synchrotron radiation spectroscopies. On the theoretical side, the precise calculation of the cross-trench CDB

adsorption energy should be carried out on large surface unit cells, or large clusters, as STM shows that at very low coverage CDB bonding induces surface buckling extending over several lattice spacings. Frustration situations associated with static dimer buckling should be specifically taken into account when one wishes to reproduce a situation of surface crowding. It could be interesting to calculate how reactivity is affected in the neighborhood of a given adspecies (e.g., a cross-trench CDB). The problem might be approached in the same manner reported by Wijdjaja and Musgrave, concerning the related case of NH₃ datively bonded to a Si dimer. They looked for the consequences of charge transfer on molecular self-assembly.²⁹ This would indeed allow a better understanding of the transition regime to high coverage, which could not be fully elucidated using the present experimental tools.

ACKNOWLEDGMENTS

The authors wish to thank Professor Gérard Boureau and Dr. Manuel Cobian for fruitful discussions about the theoretical treatment of the acrylonitrile/Si(001) system and for communicating work prior to publication. The authors are also very grateful to Dr. Coryn F. Hague for useful comments and reading the paper.

*Also at Laboratoire pour l'Utilisation du Rayonnement Electromagnétique, Centre Universitaire Paris-Sud, Batiment 209D, 91405 Orsay Cedex, France. Electronic address: roch@ccr.jussieu.fr

¹R. Wolkow, *Annu. Rev. Phys. Chem.* **50**, 413 (1999).

²S. Bent, *Surf. Sci.* **500**, 879 (2002).

³M. Filler and S. Bent, *Prog. Surf. Sci.* **73**, 1 (2003).

⁴M. Nishijima, J. Yoshinobu, H. Tsuda, and M. Onchi, *Surf. Sci.* **192**, 383 (1987).

⁵A. Mayne, A. Avery, J. Knall, T. Jones, G. Briggs, and W. Weinberg, *Surf. Sci.* **284**, 247 (1993).

⁶F. Tao, X. F. Chen, Z. H. Wang, and G. Q. Xu, *J. Am. Chem. Soc.* **124**, 7170 (2002).

⁷F. Bournel, J.-J. Gallet, S. Kubsky, G. Dufour, F. Rochet, M. Simeoni, and F. Sirotti, *Surf. Sci.* **513**, 37 (2002).

⁸M. Schwartz and R. Hamers, *Surf. Sci.* **515**, 75 (2002).

⁹C. H. Choi and M. S. Gordon, *J. Am. Chem. Soc.* **124**, 6162 (2002).

¹⁰C. Mui, M. A. Filler, S. F. Bent, and C. B. Musgrave, *J. Phys. Chem. B* **107**, 12256 (2003).

¹¹M. Cobian, V. Ilakovac, S. Carniato, N. Capron, G. Boureau, R. Hirschl, and J. Hafner, *J. Chem. Phys.* **120**, 9793 (2004).

¹²M. Cobian and G. Boureau (unpublished).

¹³J. Cho and L. Kleinman, *J. Chem. Phys.* **121**, 1557 (2004).

¹⁴J. Stöhr, *NEXAFS Spectroscopy*, 2nd ed. (Springer, New York, 1992).

¹⁵F. Tao, W. S. Sim, G. Q. Xu, and M. H. Qiao, *J. Am. Chem. Soc.* **123**, 9397 (2002).

¹⁶J. Cho and L. Kleinman, *Phys. Rev. B* **69**, 075303 (2004).

¹⁷J. Cho and L. Kleinman, *J. Chem. Phys.* **119**, 6744 (2003).

¹⁸F. Sirotti, F. Polack, J.-L. Cantin, M. Sacchi, R. Delaunay, M. Meyer, and M. Liberati, *J. Synchrotron Radiat.* **7**, 5 (2000).

¹⁹For an x-ray incidence angle θ of 54.7° the measured NEXAFS distribution is independent of the molecular orientation for threefold or higher substrate symmetry. See J. Stöhr, *NEXAFS Spectroscopy*, 2nd ed. (Springer, New York, 1998), p. 284.

²⁰A. A. Stekolnikov, J. Furthmüller, and F. Bechstedt, *Phys. Rev. B* **65**, 115318 (2002).

²¹<http://www.msg.ameslab.gov/GAMESS/GAMESS.html>

²²R. Wolkow, *Phys. Rev. Lett.* **68**, 2636 (1992).

²³Note that on Si(001), the number of surface silicon atoms is 6.8×10^{14} atoms/cm².

²⁴H. C. Kang and W. Weinberg, *Surf. Sci.* **299**, 755 (1993).

²⁵See Stöhr in Ref. 19.

²⁶The case of benzene adsorbed on the Si(001)-2×1 switching from the di- σ (butterfly) geometry to the tetra- σ one, on a time scale of ca. ≈ 1 h, is well documented [R. A. Wolkow, G. Lopinski, and D. J. Moffatt, *Surf. Sci. Lett.* **416**, L1107 (1998)].

²⁷The resulting geometry, possessing two Si-C bonds and one Si-N bond, could be thermodynamically more stable than that of the free C≡N, if the penalty induced by bond strains does not overcome the gain in making a new bond (the perturbation due to Si-N bonding should lift the degeneracy of the two π levels of the CN moiety, and give a clear NEXAFS signature).

²⁸For instance, we have no "topographic" evidence that a CDB unit can only be found on site D at high coverage.

²⁹Y. Wijdjaja and C. Musgrave, *J. Chem. Phys.* **120**, 1555 (2003).